


Commensurate vortex-core switching in magnetic nanodisks at gigahertz frequencies

Pieter Gypens¹,¹ Jonathan Leliaert¹,¹ Gisela Schütz,² and Bartel Van Waeyenberge¹,*^{1,*}

¹Department of Solid State Sciences, Ghent University, Ghent 9000, Belgium

²Max Planck Institute for Intelligent Systems, Stuttgart 70569, Germany

 (Received 16 December 2021; revised 23 February 2022; accepted 25 February 2022; published 15 March 2022)

The development of future spintronic applications requires a thorough and fundamental understanding of the magnetization dynamics. Of particular interest are magnetic nanodisks, in which the vortex state emerges as a stable spin configuration. Here, we focus on how the vortex-core polarization can be reversed periodically by an oscillating magnetic field, applied perpendicularly to the disk's surface. By means of micromagnetic simulations, we demonstrate the presence of several subharmonic switching modes, i.e., the commensurate ratio between the switching frequency of the core and the driving frequency. The underlying mechanism of this periodic behavior depends on the disk thickness. For thin disks, the core switches periodically due to resonant excitation of radial spin wave modes, while it is due to the breathing mode in the case of thick disks. However, overlap of both modes impedes periodic vortex-core switching. For thin disks, the threshold field amplitude required for periodic switching can be substantially lowered by increasing the disk diameter. For thick disks, in contrast, the diameter is less decisive for the minimal field amplitude, as only the average energy density in a central region around the vortex core is relevant to excite the breathing mode. Our results contribute to the understanding of the switching mechanisms in magnetic nanodisks, which are of technological interest due to their potential in nonvolatile memory devices.

DOI: [10.1103/PhysRevB.105.094420](https://doi.org/10.1103/PhysRevB.105.094420)

I. INTRODUCTION

In recent years, several applications have been proposed whose operation relies on the magnetization dynamics in nanostructures, ranging from nonvolatile memory devices [1–5] to logic devices [6–10], over spin-wave based communication and information processing devices [11–13]. It is therefore of fundamental importance to understand the magnetization dynamics in such structures, e.g., magnetic nanodisks in which the vortex state appears due to the competition between the short-range exchange interaction and the long-range magnetostatic interaction. In such a disk, the magnetization curls in plane in favor of the magnetostatic interaction, except at the center, where the exchange interaction starts to dominate. This central region, called the vortex core, has a radius of about 10 nm and has an out-of-plane magnetization [14,15]. The vortex state is fully characterized by two quantities: the *circulation*, which refers to the (counter)clockwise curl of the in-plane magnetization, and the *polarization* of the vortex core, which is equal to $p = -1$ for a negative out-of-plane magnetization ($m_z < 0$) and $p = +1$ for a positive out-of-plane magnetization ($m_z > 0$).

Mechanisms to reverse the circulation and core polarization in a reliable, fast, and energetically efficient manner have been studied because of their importance in the development of vortex-based memory [2,5] and logic [16,17] devices. In order to change the circulation, the original vortex core is expelled from the disk by applying an in-plane magnetic field,

after which a new core can nucleate at the border [18–20]. The circulation of the newly formed core can be controlled if the rotational symmetry of the disk is broken, e.g., via a thickness gradient [20].

The vast majority of techniques to reverse the core polarization are based on the resonant excitation of an eigenmode, as this significantly reduces the required excitation power, compared to a static out-of-plane field [21–23]. Examples of such eigenmodes are the subgigahertz gyration mode [24–26] and the multigigahertz spin wave modes, including azimuthal [27] and radial [28,29] modes.

The gyration mode is related to the circular motion of the vortex core around the center of the disk which takes place when the core has been displaced from the center. Methods to excite the gyration mode make use of linear oscillating [24], rotating [25], or pulsed [26] in-plane magnetic fields. The switching is mediated by the creation of a vortex-antivortex pair with polarization opposite to the original vortex. The antivortex subsequently annihilates with the original vortex, such that only the vortex of opposite polarization remains, thus completing the reversal [24,30,31]. This annihilation process involves the injection of a Bloch point [32], a topological singularity with vanishing magnetization at its center [33,34].

The spin wave modes are characterized by the radial and azimuthal profile of the out-of-plane oscillations of the magnetization. Excitation of azimuthal spin waves can be achieved with an oscillating in-plane magnetic field when the rotation sense matches the azimuthal mode number [27]. Similar to the gyration mode, the switching of the core polarization is mediated by the creation of a vortex-antivortex pair. Radial spin wave modes, in contrast, are excited by an oscillating

*bartel.vanwaeyenberge@ugent.be

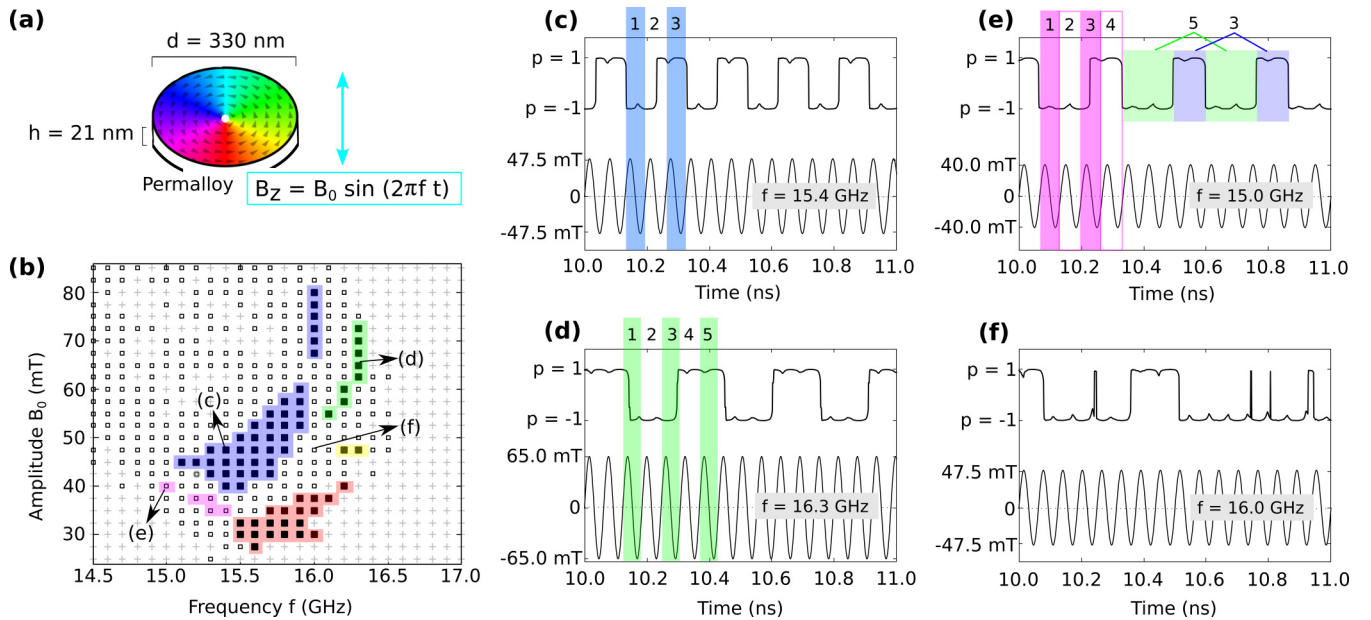


FIG. 1. (a) A circular disk is subjected to an oscillating, out-of-plane magnetic field. The color code corresponds to a counterclockwise in-plane magnetization. At the center, the magnetization points out of plane (white dot). (b) The switching diagram shows whether the polarization of the vortex core reverses (black) or not (gray). Solid squares are used to indicate periodic switching. The colors correspond to different subharmonic switching modes $1/N$, with $N = 3$ (blue), $N = 5$ (green), $N = 7$ (yellow), and $N = 9$ (red). The hybrid mode $N^* = 4$, which is a superposition of subharmonic $N = 3$ and $N = 5$, is highlighted in pink. (c)–(f) The applied field and the core polarization as a function of time for the (f, B) points indicated in the switching diagram, showing the difference between subharmonic switching modes $N = 3$ and $N = 5$, the hybrid mode $N^* = 4$, and an incommensurate mode.

out-of-plane field [28,29]. In this case, the core reverses directly due to the injection of a Bloch point. This Bloch point is created at the surface and travels through the disk towards the other surface, where it will disappear, effectively changing the polarization of the vortex core.

Besides classifying vortex-core switching via the excited mode, a distinction can be made based on the selectivity: whether the external stimulus only allows for reversals from one state to the other state (e.g., $p = -1 \rightarrow p = +1$) [25,27] or generates switching regardless of the initial core polarization, such that back and forth toggling between $p = -1$ and $p = +1$ becomes possible [24,28,29]. In this work, we focus on a special case of the latter, where the core reversals occur periodically.

Periodic vortex-core switching has already been observed in a magnetic nanocontact system during self-sustained vortex gyration, where a commensurate ratio between the gyration frequency and the switching frequency is obtained by tuning the electric current through the contact [35,36]. Alternatively, periodic switching behavior can be induced by applying an oscillating magnetic field perpendicular to the disk's surface [37,38]. As opposed to vortex gyration, here the core stays at the center of the disk, whereby the reversals occur commensurately to the frequency of the applied field. Reference [38] showed that regular switching can be achieved with a field amplitude of only a few milliteslas, albeit in double concave magnetic nanodisks which are hard to realize experimentally. The authors attribute this behavior to the fact that the energy released after a switching event is mainly dissipated to the (thick) edge part of the disk, leaving the switching process which takes place at the (thin) central part of the disk un-

affected. Nonetheless, periodic vortex-core switching in flat nanodisks was reported in Ref. [37], although at field amplitudes of at least 100 mT.

Here, we investigate how the threshold field needed to induce periodic switching in flat nanodisks can be reduced by modifying both the size and the material parameters of the disk. To this end, we vary the frequency and amplitude of the field in micromagnetic simulations to obtain switching diagrams consisting of regions of periodic and aperiodic switching and regions without switching. In contrast to Ref. [37], we focus specifically on periodic switching to reveal its origin and to demonstrate the presence of several subharmonic switching modes. The periodic behavior originates either in the resonant excitation of *radial spin wave modes* in the case of thin disks ($h < 35$ nm) or in the *breathing mode* in the case of thick disks ($h > 35$ nm). The latter occurs when the frequency of the applied field matches the rate at which the vortex core compresses and expands, i.e., the breathing mode [39].

II. METHODS

We consider circular disks with a diameter of $d = 330$ nm and a thickness of $h = 21$ nm, for which the ground state is a vortex configuration, as shown in Fig. 1(a). An oscillating magnetic field is applied perpendicularly to the surface of the disk, i.e., $\mathbf{B}(t) = B_0 \sin(2\pi f t) \mathbf{e}_z$. The switching of the core polarization is investigated for amplitudes B_0 ranging from 20 to 100 mT and frequencies f between 7 and 17 GHz. The switching diagrams are acquired by means of micromagnetic simulations using the software package MUMAX3 [40], which

numerically solves the Landau-Lifshitz-Gilbert equation. Parameters typical for permalloy are used for the saturation magnetization ($M_s = 860$ kA/m), the Gilbert-damping constant ($\alpha = 0.02$), and the exchange stiffness ($A = 13$ pJ/m). The time step is fixed at 0.1 ps. The disks are discretized into cells of $(c_x = 3 \text{ nm}) \times (c_y = 3 \text{ nm}) \times (c_z = 7 \text{ nm})$. It has been verified that the results presented in this work are independent of this larger discretization in the z direction; that is, the obtained switching diagrams are qualitatively independent of whether the simulation grid consists of seven layers with $c_z = 3$ nm or three layers with $c_z = 7$ nm.

To check whether the core switches *periodically* between $p = +1$ and $p = -1$, we track the core polarization [41] for 20 ns. The first 10 ns are sufficient for the system to exit transient states, and the subsequent 10 ns are used to determine the times t_{\min} and t_{\max} , which are the shortest and longest time intervals, respectively, for which the sign of the core polarization remains the same. In the case of periodic switching, t_{\min} and t_{\max} are equal, such that their ratio is $r = 1$. However, to account for artifacts caused by, e.g., numerical noise, we use a less strict criterion, categorizing periodic switching by $r > 0.90$. This corresponds to a difference of about 10 ps between the longest and shortest times (i.e., the equivalent of 100 time steps).

III. RESULTS

A. Subharmonic switching modes

The switching diagram in Fig. 1(b) shows how the regions of periodic switching can be classified according to their subharmonic switching mode $1/N$, with N being an *odd* number. The subharmonic switching mode indicates the ratio between the frequency at which the polarization of the vortex core reverses and the frequency of the externally applied field. We observe subharmonics for which N is equal to 3 (blue), 5 (green), 7 (yellow), and 9 (red). In Figs. 1(c) and 1(d), the applied field and the core polarization are plotted as a function of time for subharmonics 3 and 5. In addition, our micromagnetic simulations reveal so-called hybrid modes, which consist of a superposition of two subharmonics [42]. The switching frequency of the core polarization alternates between $f_p = f/N$ and $f_p = f/(N+2)$, such that a hybrid mode can effectively be regarded as an *even* subharmonic with mode number $N^* = N+1$, as illustrated in Fig. 1(e) for $N^* = 4$. However, these hybrid modes do not meet the requirement $r > 0.9$ which we impose for periodic switching (e.g., $r = 3/5$ if $N^* = 4$), and the core polarization averaged over time is nonzero, with the dominant polarization being determined by the vortex's initial state. Nonetheless, the switching behavior of hybrid modes sharply contrasts the incommensurate switching which is found when the amplitude and frequency of the external field are not tuned properly, as is clear from the example shown in Fig. 1(f). This irregular behavior encompasses both intermittent switching [37] and chaotic switching [35–37], which lie outside of the focus of this paper.

B. Excitation mechanisms

As a next step, we investigate how the switching diagrams are affected by the thickness of the disk. The disk thickness

is increased from 21 to 56 nm in steps of 7 nm by adding one additional layer at a time using the same simulation cell size as before. As shown in Fig. 2(a), the frequencies giving rise to periodic switching decrease for increasing thicknesses. To elucidate the origin of this effect, we identify the eigenfrequencies of each disk. An out-of-plane field of 30 mT is applied over the entire disk and is turned off after a period of 2 ns in order to excite spin waves. A fast Fourier transform (FFT) is performed on the z component of the magnetization m_z to transform the temporal oscillations of m_z to the frequency domain. The eigenfrequencies can be determined from the FFT power spectra, which are shown in Fig. 2(b). To exclude nonlinear effects, it has been checked that the frequency domain of the spectra (and hence the natural frequencies thus obtained) remain the same when the excitation of the spin waves is achieved by applying a block pulse of 3 mT or a sinc pulse of 5 mT amplitude (see Fig. 7 in the Appendix).

For the disks with thicknesses of 21 and 28 nm (displayed on the right in Fig. 2), periodic switching behavior is found at frequencies of about 15.8 and 14.8 GHz, respectively. These are the eigenfrequencies of the radial spin wave (RSW) modes with mode numbers $n = 2$ and $n = 3$ [43], as evidenced by the FFT amplitude spatial distribution diagrams shown in Fig. 2(c). The FFT amplitude and FFT phase profile along the cross section of the disk are shown in Fig. 8 in the Appendix.

In contrast, the thicker disks (shown on the left in Fig. 2) do not exhibit periodic switching for field amplitudes below 100 mT when the frequency of the external field matches the RSW modes. Instead, the core reverses periodically by resonant excitation of the *breathing mode* [39], which occurs at $f = 11.2$ GHz, $f = 9.7$ GHz, and $f = 8.5$ GHz for disk thicknesses of 42, 49, and 56 nm, respectively. Since the breathing mode is the periodic compression and expansion of the vortex core, the FFT amplitude diagrams in Fig. 2(c) display a peak only around the central core region, with the amplitude of the outer region being zero.

Between these two regimes, there is a transition region where the RSW mode and the breathing mode overlap. This is illustrated in Fig. 2(d), showing the eigenfrequency of the RSW mode and breathing mode as a function of disk thickness. Due to the overlap, no periodic switching behavior occurs for a 35 nm thick disk in the driving-field frequency range from 10 to 16 GHz, part of which is shown in Fig. 2(a).

C. Energy analysis

To further elaborate on the difference between periodic switching via the breathing mode and the RSW modes, we analyze how the total energy density evolves in time. For this analysis, the total energy density, which includes contributions from the exchange, magnetostatic, and Zeeman interactions, is averaged over two regions: a central region with a diameter equal to $d' = 66$ nm [purple in Fig. 3(a)] and an outer region encompassing the remaining 96% of the disk [dark green in Fig. 3(a)]. We investigate two cases [44]: (i) a 21 nm thin disk to which we apply an external out-of-plane field with frequency $f = 15.8$ GHz and amplitude $B_0 = 30.0$ mT in order to obtain subharmonic switching mode $N = 9$, shown on the left in Fig. 3(a), and (ii) a 42 nm thick disk, where the subharmonic switching mode $N = 7$ is the

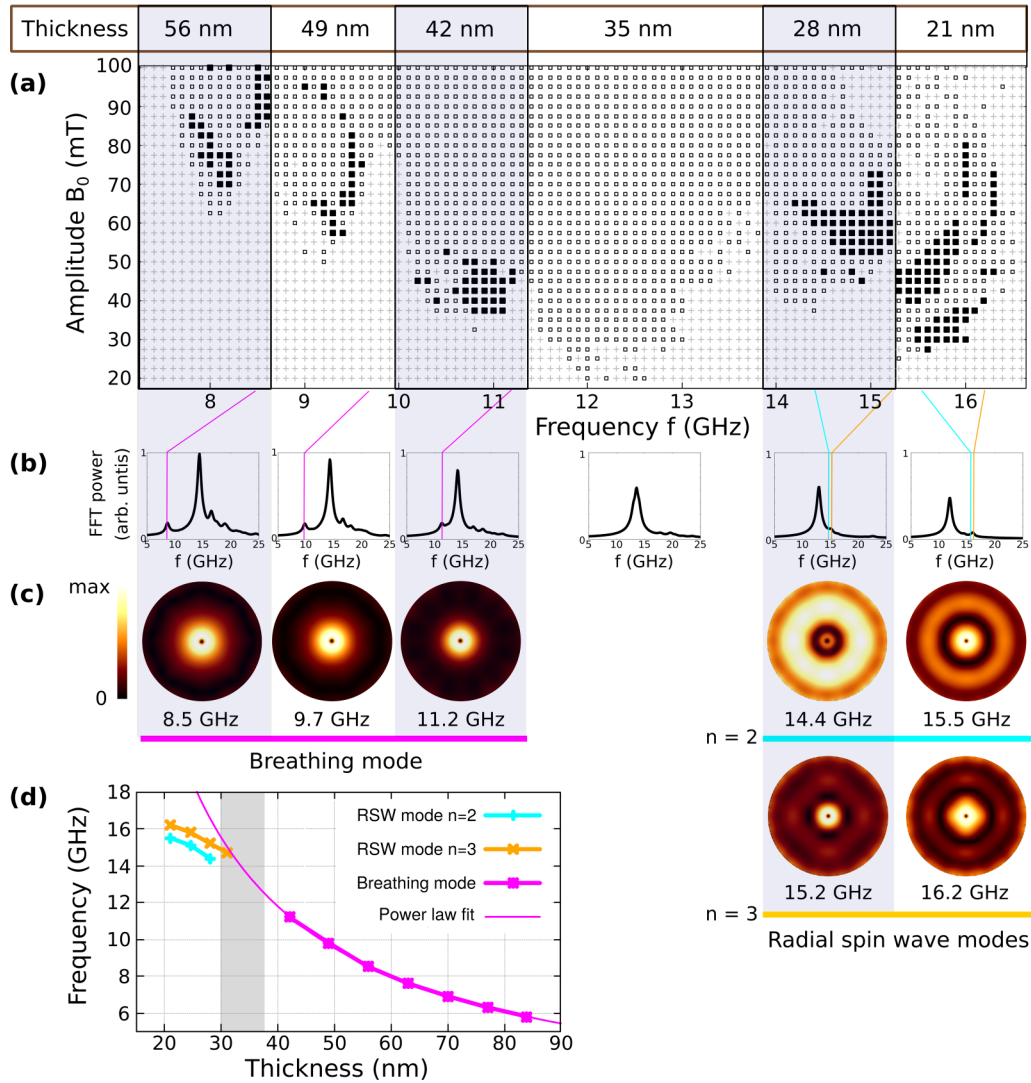


FIG. 2. (a) Switching diagrams, with the different frequency domains corresponding to different disk thicknesses, as indicated at the top. The six diagrams are joined as the regions of interest (periodic switching behavior, solid squares) are sufficiently separated by frequency for disks of such sizes. The frequencies which give rise to periodic switching increase as the disk gets thinner. (b) The FFT power spectra, normalized with the amplitude of the 56 nm thick disk. (c) The spatial distributions of the FFT amplitude at a frequency corresponding to the breathing mode (thick disks, $h > 35$ nm) or radial spin wave modes $n = 2$ and $n = 3$ (thin disks, $h < 35$ nm). (d) The thickness dependence of the eigenfrequency of the RSW modes and the breathing mode. In the crossover region, indicated by the gray band, no periodic switching is detected. The RSW modes and breathing mode could not be identified from the FFT power spectra outside the thickness regions where they are dominant and responsible for the periodic core switching, i.e., below and above the crossover region around 35 nm, respectively.

result of a field frequency $f = 11.0$ GHz and a field amplitude $B_0 = 40.0$ mT, shown on the right in Fig. 3(a). To ensure that the exchange energies can be compared, the same cell size is used for both disks [with cells of $(c_x = 3 \text{ nm}) \times (c_y = 3 \text{ nm}) \times (c_z = 7 \text{ nm})$].

For both the 21 nm thin disk and the 42 nm thick disk, the average energy density in the central region increases incrementally until a threshold above which the formation of Bloch points (BPs) is energetically allowed is reached, making it possible for the core polarization to reverse. Notably, the energy threshold displays the same value for switching induced by a static out-of-plane field (the amplitude is more than 300 mT) and chaotic switching. The existence of an

energy threshold is in agreement with the results reported in Ref. [45]. For thin disks, the reversal occurs via the injection of one BP at the surface, after which the BP travels across the disk towards the other surface, where it is expelled. The reversal in thick disks is governed by the injection of two BPs, which move in opposite directions and disappear at different surfaces, similar to the switching mechanism observed in Ref. [46]. Both the one-BP and two-BP switching mechanisms are illustrated in Fig. 3(b). However, the number of injected Bloch points is not related to which mode is excited (i.e., breathing or RSW). It is purely a result of the thickness, and we have verified that the difference between the one-BP and two-BP switching mechanisms is not due to the grid

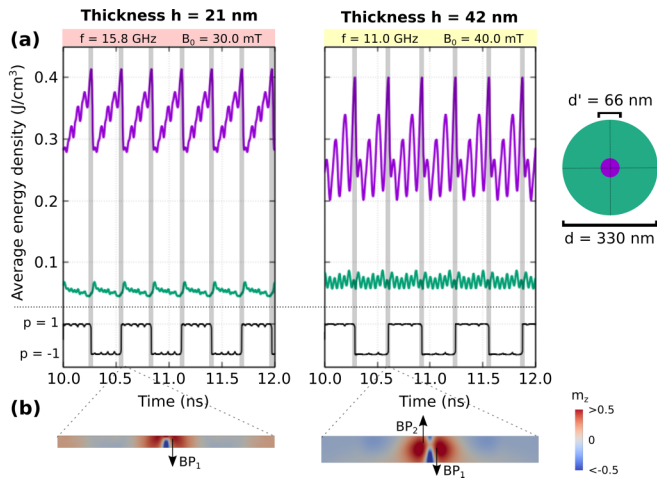


FIG. 3. (a) The average energy density in the central region (purple) and outer region (dark green) as a function of time, shown for a 21 nm thin disk (left panel) and a 42 nm thick disk (right panel). In the thin disk, spin waves transfer energy from the central region to the outer region after a core reversal, as indicated by the gray bars. In the thick disk, the oscillating field $B_0 \sin(2\pi f t) \mathbf{e}_z$ mainly pumps energy into the central region, without a transfer to the outer region, which is reminiscent of the breathing mode. (b) An illustration of the switching mechanism governing the reversal of the core polarization. The reversal occurs via the injection of either one Bloch point, labeled BP_1 , at the surface (thin disk, left) or two Bloch points, labeled BP_1 and BP_2 , in the middle (thick disk, right). The arrows indicate the direction in which the Bloch points move.

discretization. For the 21 nm thin disk, one BP is injected, irrespective of whether the simulation's grid consists of seven layers with $c_z = 3 \text{ nm}$ or three layers with $c_z = 7 \text{ nm}$.

The fact that periodic switching occurs via excitation of the RSW mode in thin disks whereas it occurs via the breathing mode in thick disks is evidenced by the time evolution of the average energy density in the outer region. For the 21 nm thin disk, the average energy density in the central region sharply drops after a reversal, where the released energy is transferred to the outer region in the form of spin waves, hence increasing the average energy density in the outer region [see the left panel in Fig. 3(a)]. The average energy density in the outer region then decreases steadily until the next switching event. This decrease is in contrast to the behavior of the 42 nm thick disk, for which the average energy density in the outer region fluctuates around a fixed value between two consecutive switching events, as shown in the right panel in Fig. 3(a). The energy of the oscillating external field is thus pumped mainly in the central region, without a transfer from the inner to the outer region. This is reminiscent of the breathing mode since this mode is due to the compressing and expanding motion of the vortex core, i.e., the central region.

D. Threshold field amplitude

So far, we have mainly focused on the frequency of the external field. This showed that periodic switching takes place when the frequency matches the breathing mode or the RSW mode, depending on the disk thickness. For potential applications, the excitation amplitude should be minimal. We

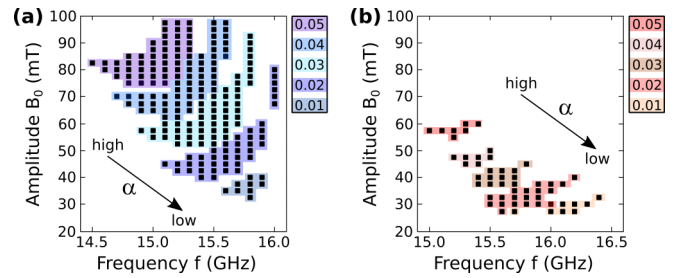


FIG. 4. The influence of the Gilbert-damping constant α on the regions with periodic switching, shown for subharmonic switching mode (a) $N = 3$ and (b) $N = 9$. The results are obtained for a 21 nm thin disk with a diameter of 330 nm.

therefore shift our attention to the field amplitude needed to induce periodic switching behavior, investigating the influence of (i) the Gilbert-damping constant, (ii) the disk size, and (iii) the inhomogeneity of the applied field.

1. Gilbert-damping constant

The influence of the Gilbert-damping constant is investigated by acquiring the switching diagram of a 21 nm thin disk for different α . Figures 4(a) and 4(b) display the (f, B) points of subharmonic switching modes $N = 3$ and $N = 9$, respectively. These results show that smaller damping gives rise to a lower threshold field, with the resonant frequencies being shifted towards slightly larger values, similar to a classical harmonic oscillator. The threshold field is lowered because the energy of the oscillating field is more effectively transferred to the disk due to the reduced energy dissipation (i.e., smaller α). However, the regions of periodic behavior are considerably smaller for $\alpha = 0.01$ than for $\alpha = 0.02$. The latter is therefore used throughout this work to trade off between energy efficiency and robustness.

2. Disk size

The effect of the thickness on the threshold field amplitude was already shown in Fig. 2. When the core switches periodically due to resonant excitation of the breathing mode, lower field amplitudes are needed for thinner disks. A similar trend is observed for the RSW mode.

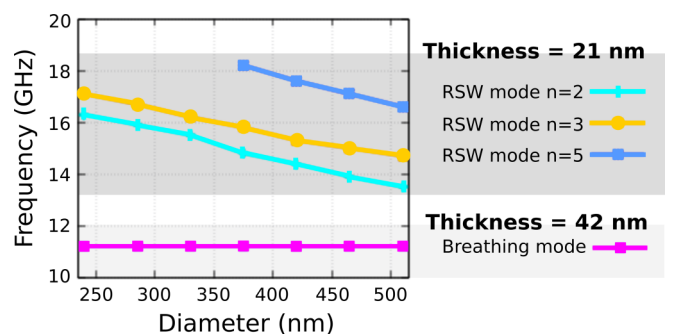


FIG. 5. The diameter dependence of the eigenfrequency of the RSW modes (for a 21 nm thin disk) and the breathing mode (for a 42 nm thick disk).

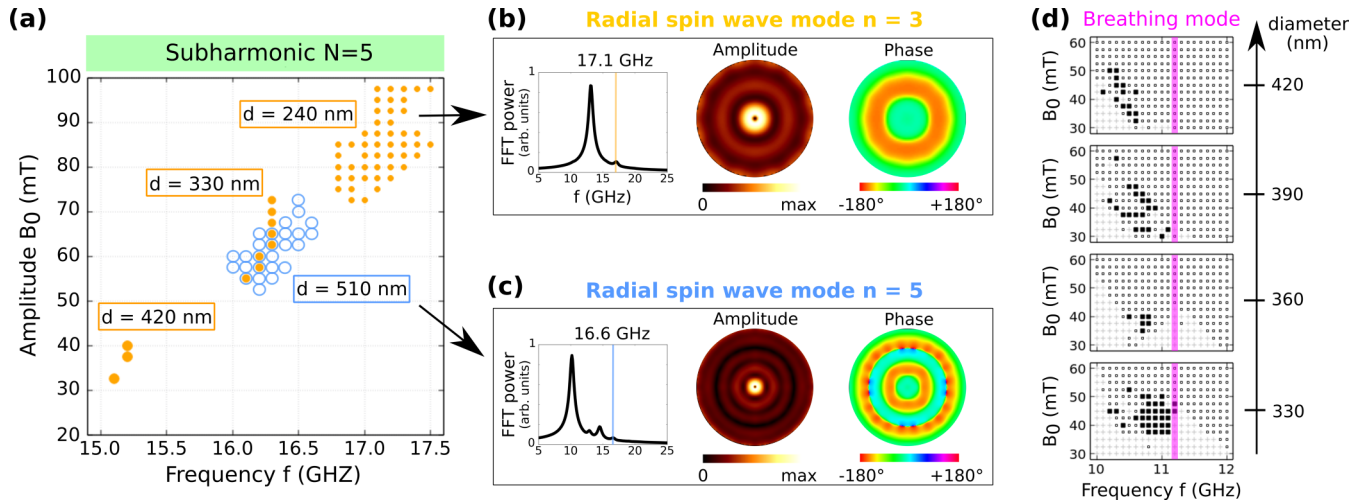


FIG. 6. (a) The influence of the disk diameter on the (f, B) points which give rise to periodic vortex-core switching for disks with a thickness of $h = 21$ nm, illustrated for subharmonic switching mode $N = 5$. (b) and (c) The FFT spectra of 240 and 510 nm diameter disks. The spatial distributions of the FFT amplitude and phase are shown at the eigenfrequency of RSW modes $n = 3$ and $n = 5$, as indicated by the orange and blue lines, respectively. (d) Switching diagrams of a 42 nm thick disk for different disk diameters, indicating no (gray), irregular (black), and periodic (solid squares) switching. For all disk diameters, periodic switching occurs between 10.5 and 11.0 GHz, slightly lower than the eigenfrequency of the breathing mode, which is equal to 11.2 GHz (pink line) for all considered diameters. The threshold field for periodic switching falls within a narrow range of 30 to 40 mT.

As a next step, we investigated the influence of the disk diameter. In Fig. 5, the eigenfrequency of the RSW modes and the breathing mode are plotted as a function of the diameter for disk thicknesses of 21 and 42 nm, respectively. A larger diameter reduces the eigenfrequency of the RSW modes, in agreement with Ref. [47], whereas the eigenfrequency of the breathing mode remains unaffected when the diameter changes.

Figure 6(a) shows the (f, B) points which give rise to subharmonic switching mode $N = 5$ in a 21 nm thin disk for different diameters. The choice of $N = 5$ is for only illustrative purposes, as the other subharmonics display the same qualitative trend. A larger diameter lowers the required field amplitude as long as the periodic behavior is caused by excitation of the same RSW mode. For instance, if the diameter is increased from $d = 240$ nm to $d = 420$ nm, the required field amplitude decreases from $B_0 = 72.5$ mT to $B_0 = 32.5$ mT, as depicted by the orange dots in Fig. 6(a). In addition, the frequency at which periodic switching occurs shifts towards lower values because the eigenfrequency of the RSW modes is lower for a larger diameter (see Fig. 5). In this case, the periodic switching is due to the excitation of the RSW mode $n = 3$, which can be seen from the spatial distributions of the FFT amplitude and phase in Fig. 6(b).

However, decreasing the required field amplitude by increasing the disk diameter does not work indefinitely. For example, for a disk with a diameter of $d = 510$ nm, no periodic switching occurs around the natural frequency of the $n = 3$ RSW mode at either lower field amplitudes or higher ones. Instead, we find that the vortex core periodically reverses for frequencies close to the natural frequency of the $n = 5$ RSW mode, the spatial distributions of which are shown in Fig. 6(c). The periodic switching happens at a field of more than 50 mT, as indicated by the blue dots in Fig. 6(a). Despite the larger diameter, the required field has not de-

creased compared to the $d = 420$ nm disk. This indicates that the energy pumped into the outer edges of the system is no longer transferred efficiently to the core region, e.g., due to damping. As a consequence, the average energy density in the core region does not reach the threshold value necessary for the formation of a Bloch point (see the left panel in Fig. 3). A minimal field must therefore be applied in order to induce (periodic) switching, which is about 30 mT for the material parameters outlined above.

A similar analysis can be made for thick disks, in which the periodic switching is related to the breathing mode. We focus on disks with a thickness of $h = 42$ nm and a diameter ranging from 330 to 420 nm. For all disk diameters, the regions of periodic switching are expected to occur near a frequency of 11.2 GHz, i.e., the eigenfrequency of the breathing mode, which remains constant when the diameter changes (see Fig. 5). The results shown in Fig. 6(d) corroborate this picture: periodic switching occurs at frequencies between 10.5 and 11.0 GHz, slightly lower than the eigenfrequency of the breathing mode. During the excitation of the breathing mode, the energy of the oscillating external field is mainly pumped in the central region. Because this central region is independent of the total disk diameter, the threshold field of periodic switching barely varies, ranging from 30 to 40 mT for all considered diameters. This is in sharp contrast to thin disks, where the required field is halved by increasing the diameter from 330 to 420 nm [see Fig. 6(a)].

3. Inhomogeneous fields

So far, the field has been applied homogeneously over the entire disk. Additional simulations show that periodic switching also emerges when the field is applied in only the central region around the core. Compared to the homogeneous case, however, the threshold field to induce periodic core reversals

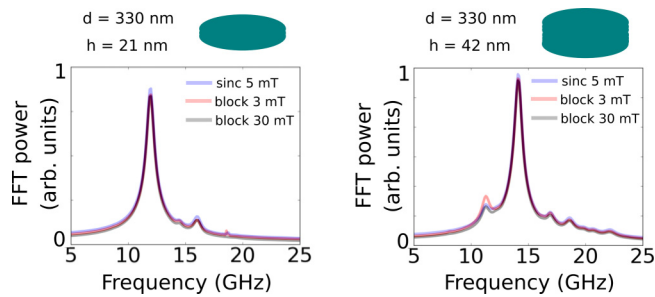


FIG. 7. The frequency domain of the FFT power spectrum is not affected by the field pulse or field amplitude used to excite spin waves. The FFT power has been rescaled to allow for a comparison of the different pulse types.

in a 21 nm thin disk with diameter $d = 330$ nm and central region $d' = 66$ nm increases from 30 to 40 mT (subharmonic switching mode $N = 9$) and from 40 to 50 mT (subharmonic switching mode $N = 3$). This larger field amplitude is needed to compensate for the energy transfer from the outer to the central region.

In a 42 nm thick disk, the switching is due to excitation of the breathing mode, for which only the average energy density in the central region is relevant. This means that the minimal field amplitude should remain constant, irrespective of whether the field is applied over the entire disk or over only the central region. This hypothesis is confirmed by our simulations, yielding a threshold field of about 40 mT for all cases.

IV. CONCLUSION

We showed that the polarization of the vortex core can be reversed periodically in magnetic nanodisks by applying an oscillating out-of-plane field. Two different regimes could be identified. The frequency of the field should be tuned to the eigenfrequency of the radial spin wave modes in the case of thin disks (<35 nm) or the eigenfrequency of the breathing mode in the case of thick disks (>35 nm). For thin disks, the threshold field amplitude required for periodic switching can be substantially lowered by increasing the disk diameter d (from about 70 mT for $d = 240$ nm to about 30 mT for $d = 420$ nm). For thick disks, in contrast, the disk diameter is less decisive for the minimal field amplitude, as only the average energy density in a central region around the vortex core is relevant to excite the breathing mode. Our results contribute to the understanding of the switching mechanisms

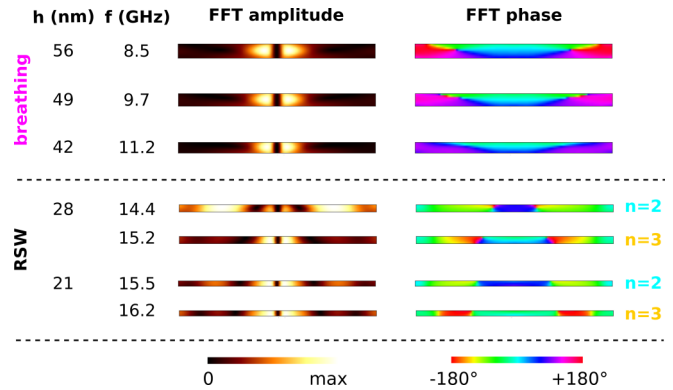


FIG. 8. The FFT amplitude and FFT phase profile along the cross section of the disk, shown for the modes responsible for periodic vortex-core switching, i.e., the breathing mode in thick disks ($h > 35$ nm) and the radial spin wave (RSW) modes in thin disks ($h < 35$ nm). The disk diameter is 330 nm.

in magnetic nanodisks, which are of technological interest due to their potential in nonvolatile memory devices.

ACKNOWLEDGMENTS

This work was supported by the Fonds Wetenschappelijk Onderzoek (FWO-Vlaanderen) with senior postdoctoral research fellowship 12W7622N (J.L.).

APPENDIX

The eigenfrequencies of a disk are determined from the FFT power spectrum. To obtain such a spectrum, spin waves are excited, and the temporal oscillations of m_z are transformed to the frequency domain by performing a fast Fourier transform. The robustness of this method has been validated by using different field pulses and field amplitudes for the excitation of spin waves. For the investigated disks, the frequency domain of the FFT spectrum (and hence the eigenfrequencies thus obtained) is independent of whether we use a 2 ns block pulse of 3 mT, a 2 ns block pulse of 30 mT, or a sinc pulse of 5 mT amplitude. This is illustrated in Fig. 7 for a 330 nm diameter disk with thickness $h = 21$ nm (left panel) and $h = 42$ nm (right panel).

The FFT amplitude and FFT phase profile along the cross section of the disk are displayed in Fig. 8 for several disk thicknesses. No modes along the disk axis could be identified.

- [1] S. Zhang and Z. Li, Roles of Nonequilibrium Conduction Electrons on the Magnetization Dynamics of Ferromagnets, *Phys. Rev. Lett.* **93**, 127204 (2004).
- [2] S. Bohlens, B. Krüger, A. Drews, M. Bolte, G. Meier, and D. Pfannkuche, Current controlled random-access memory based on magnetic vortex handedness, *Appl. Phys. Lett.* **93**, 142508 (2008).
- [3] S. Parkin, M. Hayashi, and L. Thomas, Magnetic domain-wall racetrack memory, *Science* **320**, 190 (2008).

- [4] J. Sampaio, V. Cros, S. Rohart, A. Thiaville, and A. Fert, Nucleation, stability and current-induced motion of isolated magnetic skyrmions in nanostructures, *Nat. Nanotech.* **8**, 839 (2013).
- [5] L. D. Geng and Y. M. Jin, Magnetic vortex racetrack memory, *J. Magn. Magn. Mater.* **423**, 84 (2017).
- [6] J. Wang, H. Meng, and J.-P. Wang, Programmable spintronics logic device based on a magnetic tunnel junction element, *J. Appl. Phys.* **97**, 10D509 (2005).

- [7] D. A. Allwood, G. Xiong, C. C. Faulkner, D. Atkinson, D. Petit, and R. P. Cowburn, Magnetic domain-wall logic, *Science* **309**, 1688 (2005).
- [8] A. Imre, G. Csaba, L. Ji, A. Orlov, G. Bernstein, and W. Porod, Majority logic gate for magnetic quantum-dot cellular automata, *Science* **311**, 205 (2006).
- [9] X. Zhang, G. Zhao, H. Fangohr, J. P. Liu, W. Xia, J. Xia, and F. Morvan, Skyrmion-skyrmion and skyrmion-edge repulsions in skyrmion-based racetrack memory, *Sci. Rep.* **5**, 7643 (2015).
- [10] Z. Luo, A. Hrabec, T. P. Dao, G. Sala, S. Finizio, J. Feng, S. Mayr, J. Raabe, P. Gambardella, and L. J. Heyderman, Current-driven magnetic domain-wall logic, *Nature (London)* **579**, 214 (2020).
- [11] G. Dieterle, J. Förster, H. Stoll, A. S. Semisalova, S. Finizio, A. Gangwar, M. Weigand, M. Noske, M. Fähnle, I. Bykova, J. Gräfe, D. A. Bozhko, H. Y. Musiienko-Shmarova, V. Tiberkevich, A. N. Slavin, C. H. Back, J. Raabe, G. Schütz, and S. Wintz, Coherent Excitation of Heterosymmetric Spin Waves with Ultrashort Wavelengths, *Phys. Rev. Lett.* **122**, 117202 (2019).
- [12] J. Han, P. Zhang, J. T. Hou, S. A. Siddiqui, and L. Liu, Mutual control of coherent spin waves and magnetic domain walls in a magnonic device, *Science* **366**, 1121 (2019).
- [13] W. Yu, J. Lan, and J. Xiao, Magnetic Logic Gate Based on Polarized Spin Waves, *Phys. Rev. Appl.* **13**, 024055 (2020).
- [14] J. Miltat and A. Thiaville, Vortex cores—Smaller than small, *Science* **298**, 555 (2002).
- [15] A. Wachowiak, J. Wiebe, M. Bode, O. Pietzsch, M. Morgenstern, and R. Wiesendanger, Direct observation of internal spin structure of magnetic vortex cores, *Science* **298**, 577 (2002).
- [16] H. Jung, Y.-S. Choi, K.-S. Lee, D.-S. Han, Y.-S. Yu, M.-Y. Im, P. Fischer, and S.-K. Kim, Logic operations based on magnetic-vortex-state networks, *ACS Nano* **6**, 3712 (2012).
- [17] D. Kumar, S. Barman, and A. Barman, Magnetic vortex based transistor operations, *Sci. Rep.* **4**, 4108 (2014).
- [18] Y. Gaididei, D. D. Sheka, and F. G. Mertens, Controllable switching of vortex chirality in magnetic nanodisks by a field pulse, *Appl. Phys. Lett.* **92**, 012503 (2008).
- [19] R. Antos and Y. Otani, Simulations of the dynamic switching of vortex chirality in magnetic nanodisks by a uniform field pulse, *Phys. Rev. B* **80**, 140404(R) (2009).
- [20] V. Uhlíř, M. Urbánek, L. Hladík, J. Spousta, M.-Y. Im, P. Fischer, N. Eibagi, J. J. Kan, E. E. Fullerton, and T. Šikola, Dynamic switching of the spin circulation in tapered magnetic nanodisks, *Nat. Nanotechnol.* **8**, 341 (2013).
- [21] T. Okuno, K. Shigeto, T. Ono, K. Mibu, and T. Shinjo, MFM study of magnetic vortex cores in circular permalloy dots: Behavior in external field, *J. Magn. Magn. Mater.* **240**, 1 (2002).
- [22] A. Thiaville, J. M. García, R. Dittrich, J. Miltat, and T. Schrefl, Micromagnetic study of Bloch-point-mediated vortex core reversal, *Phys. Rev. B* **67**, 094410 (2003).
- [23] R. Wang and X. Dong, Sub-nanosecond switching of vortex cores using a resonant perpendicular magnetic field, *Appl. Phys. Lett.* **100**, 082402 (2012).
- [24] B. Van Waeyenberge, A. Puzic, H. Stoll, K. Chou, T. Tylliszczak, R. Hertel, M. Fähnle, H. Brückl, K. Rott, G. Reiss, I. Neudecker, D. Weiss, C. H. Back, and G. Schütz, Magnetic vortex core reversal by excitation with short bursts of an alternating field, *Nature (London)* **444**, 461 (2006).
- [25] M. Curcic, B. Van Waeyenberge, A. Vansteenkiste, M. Weigand, V. Sackmann, H. Stoll, M. Fähnle, T. Tylliszczak, G. Woltersdorf, C. H. Back, and G. Schütz, Polarization Selective Magnetic Vortex Dynamics and Core Reversal in Rotating Magnetic Fields, *Phys. Rev. Lett.* **101**, 197204 (2008).
- [26] M. Weigand, B. Van Waeyenberge, A. Vansteenkiste, M. Curcic, V. Sackmann, H. Stoll, T. Tylliszczak, K. Kaznatcheev, D. Bertwistle, G. Woltersdorf, C. H. Back, and G. Schütz, Vortex Core Switching by Coherent Excitation with Single In-Plane Magnetic Field Pulses, *Phys. Rev. Lett.* **102**, 077201 (2009).
- [27] M. Kammerer, M. Weigand, M. Curcic, M. Noske, M. Sproll, A. Vansteenkiste, B. Van Waeyenberge, H. Stoll, G. Woltersdorf, C. H. Back, and G. Schuetz, Magnetic vortex core reversal by excitation of spin waves, *Nat. Commun.* **2**, 279 (2011).
- [28] M.-W. Yoo, J. Lee, and S.-K. Kim, Radial-spin-wave-mode-assisted vortex-core magnetization reversals, *Appl. Phys. Lett.* **100**, 172413 (2012).
- [29] X. Dong, Z. Wang, and R. Wang, Deep sub-nanosecond reversal of vortex cores confined in a spin-wave potential well, *Appl. Phys. Lett.* **104**, 112413 (2014).
- [30] R. Hertel, S. Gliga, M. Fähnle, and C. M. Schneider, Ultrafast Nanomagnetic Toggle Switching of Vortex Cores, *Phys. Rev. Lett.* **98**, 117201 (2007).
- [31] Y. Liu, S. Gliga, R. Hertel, and C. M. Schneider, Current-induced magnetic vortex core switching in a permalloy nanodisk, *Appl. Phys. Lett.* **91**, 112501 (2007).
- [32] R. Hertel and C. M. Schneider, Exchange Explosions: Magnetization Dynamics during Vortex-Antivortex Annihilation, *Phys. Rev. Lett.* **97**, 177202 (2006).
- [33] E. Feldtkeller, Continuous and Singular Micromagnetic Configurations, *IEEE Transactions on Magnetics* **53**, 0700308 (2017).
- [34] W. Döring, Point singularities in micromagnetism, *J. Appl. Phys.* **39**, 1006 (1968).
- [35] S. Petit-Watelot, J.-V. Kim, A. Ruotolo, R. M. Otxoa, K. Bouzehouane, J. Grollier, A. Vansteenkiste, B. Van de Wiele, V. Cros, and T. Devolder, Commensurability and chaos in magnetic vortex oscillations, *Nat. Phys.* **8**, 682 (2012).
- [36] M.-W. Yoo, D. Rontani, J. Létang, S. Petit-Watelot, T. Devolder, M. Sciamanna, K. Bouzehouane, V. Cros, and J.-V. Kim, Pattern generation and symbolic dynamics in a nanocontact vortex oscillator, *Nat. Commun.* **11**, 601 (2020).
- [37] O. V. Pylypovskiy, D. D. Sheka, V. P. Kravchuk, F. G. Mertens, and Y. Gaididei, Regular and chaotic vortex core reversal by a resonant perpendicular magnetic field, *Phys. Rev. B* **88**, 014432 (2013).
- [38] X.-P. Ma, M.-X. Cai, P. Li, J.-H. Shim, H.-G. Piao, and D.-H. Kim, Periodic vortex core switching in curved magnetic nanodisk, *J. Magn. Magn. Mater.* **502**, 166481 (2020).
- [39] M. Mruczkiewicz, M. Krawczyk, and K. Y. Guslienko, Spin excitation spectrum in a magnetic nanodot with continuous transitions between the vortex, Bloch-type skyrmion, and Néel-type skyrmion states, *Phys. Rev. B* **95**, 094414 (2017).
- [40] A. Vansteenkiste, J. Leliaert, M. Dvornik, M. Helsen, F. Garcia-Sanchez, and B. Van Waeyenberge, The design and verification of MuMax3, *AIP Adv.* **4**, 107133 (2014).
- [41] The core polarization p is determined by a built-in feature of MUMAX3, which returns the out-of-plane magnetization of

- the cell with the largest $|m_z|$. In our simulations, the largest perpendicular magnetization component is always $|m_z| > 0.75$, with the vortex core staying at the disk center upon switching.
- [42] The periodic switching reported in Ref. [38] is, according to our classification of periodicity, a hybrid mode which alternates regularly between the subharmonics with mode number $N = 5$ and $N = 7$.
- [43] M. Buess, T. P. J. Knowles, R. Höllinger, T. Haug, U. Krey, D. Weiss, D. Pescia, M. R. Scheinfein, and C. H. Back, Excitations with negative dispersion in a spin vortex, *Phys. Rev. B* **71**, 104415 (2005).
- [44] See Supplemental Material at <http://link.aps.org/supplemental/10.1103/PhysRevB.105.094420> for movies of the two cases.
- [45] S. Gliga, Y. Liu, and R. Hertel, Energy thresholds in the magnetic vortex core reversal, *J. Phys.: Conf. Ser.* **303**, 012005 (2011).
- [46] P. Wohlhüter, M. T. Bryan, P. Warnicke, S. Gliga, S. E. Stevenson, G. Heldt, L. Saharan, A. K. Suszka, C. Moutafis, R. V. Chopdekar *et al.*, Nanoscale switch for vortex polarization mediated by Bloch core formation in magnetic hybrid systems, *Nat. Commun.* **6**, 7836 (2015).
- [47] K. Vogt, O. Sukhostavets, H. Schultheiss, B. Obry, P. Pirro, A. A. Serga, T. Sebastian, J. Gonzalez, K. Y. Guslienko, and B. Hillebrands, Optical detection of vortex spin-wave eigenmodes in microstructured ferromagnetic disks, *Phys. Rev. B* **84**, 174401 (2011).